

Damped 2DOF Model of MIL-S-901D Medium-Weight Shock Machine Test

J. Edward Alexander, BAE Weapon Systems, Minneapolis, Minnesota

A two-degree-of-freedom (2DOF) lumped mass analytical model of the MIL-S-901D high-impact, medium-weight shock machine (MWSM)⁵ has been updated to include damping. An initial nondamped analytical model was developed by Welsh and Sanders.¹ MWSM test data taken by FMC Corporation⁴ and testing conducted by the Naval Research Laboratory (NRL)³ has indicated that critical damping in the range of 4-5% exists during the test event. Beyond the addition of damping, the relationship of anvil table “kick-off” velocity as a function of hammer impact velocity has been further explored. A relationship presented by NRL³ indicated that initial anvil table velocity is 54.5% of hammer impact velocity averaged over all hammer drop heights. This relationship corresponds to a 52% loss of kinetic energy as a result of hammer impact, a significant amount. FMC testing data correlated more closely to no loss of kinetic energy due to hammer impact. Additional anvil table kick-off velocity relationships are presented here based on the FMC test data and also no loss of energy due to hammer impact.

A MATLAB function was developed based on the 2DOF MWSM damped equations of motion. The MATLAB function returns time-based displacements, velocities and accelerations for the equipment and the anvil table up to the point that the anvil table hits the travel stops of the machine. The function also returns a shock response spectrum (SRS) of the equipment acceleration during the “up-shock” event. The model makes no attempt to predict “rebound shock” to the equipment when the anvil table hits the stops of the machine.

While a lumped mass 2DOF model cannot predict equipment response with the degree of accuracy to that of a transient multi-degree-of-freedom (MDOF), multi-frequency, finite-element model of the anvil table and the equipment, the 2DOF model does provide a quick and easy means to approximate the transient acceleration that the equipment will experience during a MWSM shock test. The 2DOF model transient response could, for example, be used to

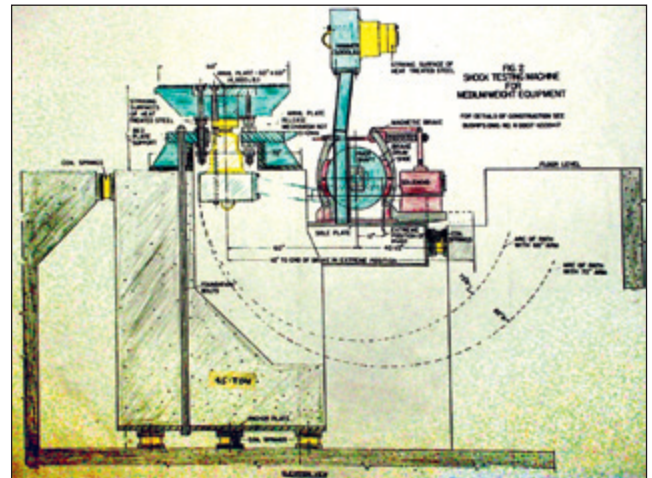


Figure 1. MIL-S-901D medium-weight shock machine.

terminate a base input acceleration to a more detailed MDOF model of the equipment. This could be especially helpful, for example, during the preliminary design phase of equipment development when numerous design changes must be evaluated rapidly.

Description of MWSM

The MIL-S-901D medium-weight shock machine consists of a 3,000-pound pendulum hammer, a 4,400-pound anvil table that the test equipment is mounted to and a 45-ton, reactive mass mounted to the floor with a series of coil springs. A standard test consists of raising the pendulum hammer above horizontal to a specified drop height h and releasing it to rotate underneath the anvil table and strike it from below. The hammer impact results in a nearly instant vertical “kick-off” velocity of the anvil table, which can travel freely until the table contacts the stops of the machine.

Equipment mounted to the anvil table experiences a shock acceleration that is transmitted by the anvil table kick-off velocity through a specified number of N flexible car-building channels that are mounted to two ship-building channels. The N car-building channels are specified based on the span of the equipment mounting locations (Dimension A) and the weight of the equipment to achieve a frequency in the range of the hull of a ship.

The test consists of releasing the hammer, which is raised above horizontal by h feet, resulting in a hammer-to-anvil table contact velocity of approximately $\sqrt{2gh}$. The original objective of the test was to achieve an initial kick-off velocity of the anvil table of six feet per second. After hammer impact, the anvil table travels upward until it hits the stops of the machine, which are set to either 3.0 in or 1.5 in for a standard MIL-S-901D test. When the anvil table contacts the stops, the impact results in a rebound shock, the severity of which depends on phasing between the anvil table and equipment motions at the point of impact. A schematic of the MWSM is shown in Figure 1.

Damped 2DOF MWSM Model

The initial 2DOF analytical model was developed by Welsh and Saunders.¹ In this model, the shock machine was assumed to have no damping ($\zeta = 0$). The same nondamped model was also described by Scavuzzo and Pusey.⁶ The presence of damping was observed during testing conducted by the Naval Research Laboratory³ and by FMC Corp.⁴ The analytical 2DOF model documented

Nomenclature

0-	Instant in time just prior to hammer impact
0+	Instant in time just after hammer impact
2DOF	Two degrees of freedom
B	Rigid body velocity
Dim A	Dimension A prescribed for MWSM test by MIL-S-901D
EOM	Equations of motion
g	Acceleration due to gravity
h	Hammer drop height
L	Energy loss
MDOF	Multi degree of freedom
MIL-S-901D	Military Standard 901D
MWSM	Medium-weight shock machine
N	Number of car-building channels used in test
nel	No energy loss
NRL	U.S. Naval Research Laboratory
R	Mass ratio of anvil table to hammer masses
SDOF	Single degree of freedom
SRS	Shock Response Spectrum
ζ	Percent of critical damping expressed as fraction
ω	Frequency in radians/sec
ω_d	Damped frequency in radians/sec

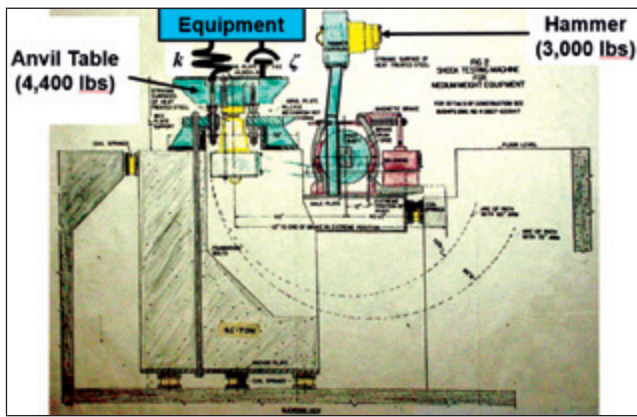


Figure 2. Equipment on medium-weight shock machine.

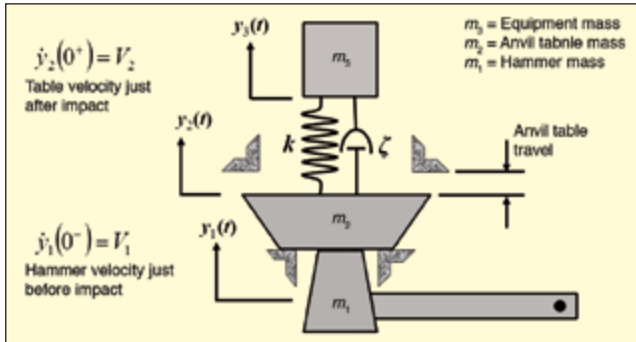


Figure 3. Medium-weight shock machine 2DOF model.

here includes damping represented as a percent of critical damping. As illustrated in Figures 2 and 3, the equipment is represented as a single lumped mass. The hammer, anvil table and equipment masses are indicated by m_1 , m_2 and m_3 , respectively, with coordinates y_1 , y_2 and y_3 , respectively, in Figure 3. The stiffness k represents the combined stiffness of N car-building channels that support the equipment. Damping is represented as a percent of critical damping, indicated by ζ . The system, initially at rest, is excited by the hammer impact to the underside of the anvil table with an upward velocity of V_1 just prior to impact, designated as time, $t = 0^-$. The impact results in an initial “kick-off” velocity of the anvil table, designated as an initial condition V_2 in the analytical model at time, $t = 0^+$, just after hammer impact.

The relationship of the anvil table kick-off velocity as a function of the hammer impact velocity, $V_2 = f(V_1)$, is developed from conservation of momentum and conservation of energy given by Eqs. 1 and 2, respectively:

Conservation of momentum:

$$m_1 V_1 = m_1 \dot{y}_1(0^+) + m_2 V_2 \quad (1)$$

Conservation of energy:

$$\frac{1}{2} m_1 V_1^2 = \frac{1}{2} m_1 \dot{y}_1^2(0^+) + \frac{1}{2} m_2 V_2^2 + L \left(\frac{1}{2} m_1 V_1^2 \right) \quad (2)$$

The velocity ratio V_2/V_1 , given by Eq. 3, is solved from Eqs. 1 and 2:

$$\frac{V_2}{V_1} = \frac{R \pm \sqrt{R^2 - L(R^2 + R)}}{(R^2 + R)} \quad (3)$$

where $R = m_2/m_1$ and L is the energy loss during the collision.

A velocity ratio V_2/V_1 was determined by testing performed by Clements at the Naval Research Laboratory.³ Figure 4 is a plot of the data from Ref. 3, where a straight line fit of the data is given by Eq. 4:

$$V_2 = 0.545 V_1 \quad (4)$$

When L is solved in Eq. 3 using Eq. 4, the resulting energy loss is L is a significant 52.4%. It is noted that if Eq. 4 holds, the instant after the hammer strikes anvil table, the hammer continues upward with a positive upward velocity. High-speed video was taken by BAE Systems to determine if this was the case. The video showed

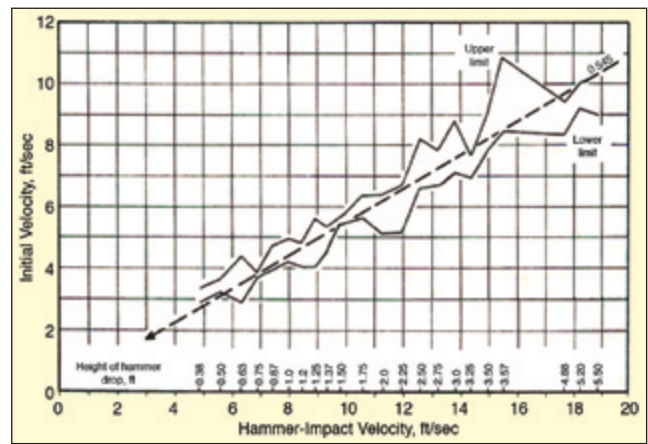


Figure 4. Correlation of anvil table kickoff velocity to hammer height.³

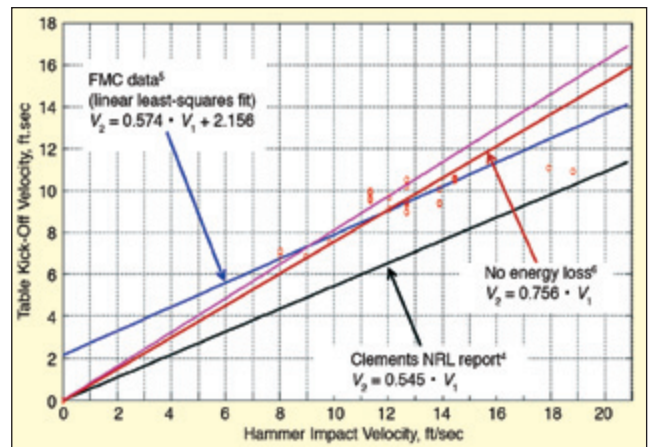


Figure 5. Anvil table kickoff velocity to hammer impact velocity correlation.

that the hammer did not continue to move upward after impact. The hammer appeared to stop instantly at impact and immediately fall downward, away from anvil table. As an additional system check, $V_2 = f(V_1)$ was determined from FMC MWSM test data,⁵ resulting in a relationship for V_2 given by Eq. 5, which is a linear least-squares fit through the FMC data points in Figure 5.

$$V_2 = 0.574 V_1 + 2.156 \text{ (ft / sec)} \quad (5)$$

A third option is offered assuming there is no loss of kinetic energy due to the collision. The resulting relationship for no energy loss is given by Eq. 6.

$$V_2 = 0.756 V_1 \quad (6)$$

The three relationships for $V_2 = f(V_1)$ represented by Eqs. 4, 5 and 6 are plotted in Figure 5. The individual data points plotted correspond to FMC test results. The “no energy loss” relationship (Eq. 6) appears to also be consistent with the individual FMC data points. The relationship indicated by Eq. 4 does not fit the FMC plotted data, except possibly a at high hammer impact velocities above 18 ft/sec. Inasmuch as the FMC linear data fit given by Eq. 5 does not go through zero for zero hammer velocity, it is suggested that below hammer velocities of 8 ft/sec that Eq. 6 be used.

Development of MWSM Damped Equations of Motion

The damped equations of motion (EOM) were developed with an approach similar to those used in References 1 and 2. Damping has been observed during MWSM shock tests as documented in References 3 and 4. The EOMs developed herein include damping characterized by a percent of critical damping for the entire system. The equations of motion are developed for equipment and the anvil table immediately after hammer impact has occurred. Both the equipment and the anvil table masses are placed into dynamic force equilibrium by setting $\Sigma Forces = 0$ as illustrated in Figure 6. The resulting equations of motion for the equipment and the anvil table are given by Eqs. 7 and 8, respectively:

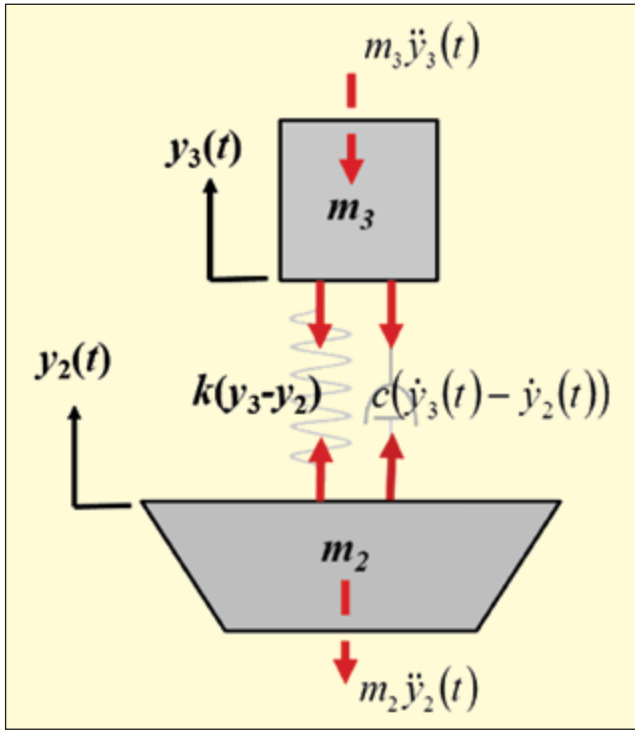


Figure 6. Forces on equipment and anvil table.

$$m_3 \ddot{y}_3(t) + c[\dot{y}_3(t) - \dot{y}_2(t)] + k[y_3(t) - y_2(t)] = 0 \quad (7)$$

$$m_2 \ddot{y}_2(t) - c[\dot{y}_3(t) - \dot{y}_2(t)] - k[y_2(t) - y_3(t)] = 0 \quad (8)$$

The initial conditions are given by Eq.9, where time = 0 corresponds to hammer impact. V_2 is the table velocity immediately after impact (0^+):

$$\begin{aligned} y_2(0) = y_3(0) = \dot{y}_3(0) = 0 \\ \dot{y}_2(0^+) = V_2 \end{aligned} \quad (9)$$

Damped sinusoidal motion is the assumed solution for the anvil table and the equipment given by Eqs. 10 and 11. Equations include ζ (percent of critical damping), rather than the discrete damping constant c as indicated in Figure 6. The damped frequency is given by Eq.12.

$$y_2(t) = A_2 e^{-\zeta \omega t} \sin(\omega_d t) \quad (10)$$

$$y_3(t) = A_3 e^{-\zeta \omega t} \sin(\omega_d t) \quad (11)$$

$$\omega_d = \sqrt{1 - \zeta^2} \omega \quad (12)$$

To determine the non-damped natural frequencies for the 2DOF system, the nondamped sinusoidal displacement equations given by Eqs. 13 and 14 are substituted into the equations of motion, Eqs. 7 and 8. This results in two expressions for the amplitude ratio A_2/A_3 given by Eqs. 15 and 16. The amplitude ratio given by Eq. 15 is determined from Eq. 7, and Eq. 16 is determined from Eq. 8.

$$y_2(t) = A_2 \sin(\omega t) \quad (13)$$

$$y_3(t) = A_3 \sin(\omega t) \quad (14)$$

$$\frac{A_2}{A_3} = \frac{k}{(k - \omega^2 m_2)} \quad (15)$$

$$\frac{A_2}{A_3} = \frac{(k - \omega^2 m_3)}{k} \quad (16)$$

The non-damped natural frequencies for the 2DOF system are

determined by equating A_2/A_3 in Eqs. 15 and 16 and moving all terms to the right-hand side of the equation, which gives Eq. 17:

$$0 = \omega^2 \left(\frac{-k(m_2 + m_3)}{m_2 m_3} + \omega^2 \right) \quad (17)$$

Equation 17 has two solutions for ω^2 , Eqs. 18 and 19, both of which are valid for the MWSM system.

$$\omega_1^2 = 0 \quad (18)$$

and

$$\omega_2^2 = \frac{k(m_2 + m_3)}{m_2 m_3} \quad (19)$$

Equation 18 is a rigid-body mode, which represents the upward translation of the equipment and the anvil table until the anvil table contacts the machine stops. Equation 19 corresponds to the elastic mode, which represents the relative motion of the equipment and the anvil table as the entire system translates upward until the anvil table contacts the stops of the machine. Both are valid modes for this system. However, with the presence of a rigid-body mode, another term must be added to the assumed sinusoidal motion of the anvil table and the equipment given by Eqs. 10 and 11. The additional term is to account for the rigid-body motion corresponding to $\omega = 0$, resulting in modified equations of motion given by Eqs. 20 and 21, where B is the rigid-body velocity:

$$y_2(t) = A_2 e^{-\zeta \omega t} \sin(\omega_d t) + Bt \quad (20)$$

$$y_3(t) = A_3 e^{-\zeta \omega t} \sin(\omega_d t) + Bt \quad (21)$$

The velocities and accelerations for the anvil table and the equipment are determined from the first and second derivatives for Eqs. 20 and 21, respectively. The velocity and acceleration of the anvil table are given by Eqs. 22 and 23, respectively:

$$\dot{y}_2(t) = A_2 e^{-\zeta \omega t} [\omega_d \cos(\omega_d t) - \zeta \omega \sin(\omega_d t)] + B \quad (22)$$

$$\ddot{y}_2(t) = 2A_2 \omega^2 e^{-\zeta \omega t} \left[\left(\zeta^2 - \frac{1}{2} \right) \sin(\omega_d t) - \zeta \sqrt{1 - \zeta^2} \cos(\omega_d t) \right] \quad (23)$$

The velocity and acceleration of the equipment are given by Eqs. 24 and 25, respectively.

$$\dot{y}_3(t) = A_3 e^{-\zeta \omega t} [\omega_d \cos(\omega_d t) - \zeta \omega \sin(\omega_d t)] + B \quad (24)$$

$$\ddot{y}_3(t) = 2A_3 \omega^2 e^{-\zeta \omega t} \left[\left(\zeta^2 - \frac{1}{2} \right) \sin(\omega_d t) - \zeta \sqrt{1 - \zeta^2} \cos(\omega_d t) \right] \quad (25)$$

These motions are valid for the “up-shock” portion of the shock test only. When the anvil table contacts the stops of the machine, the equations are no longer valid. Amplitudes of motion A_2 and A_3 are determined from the initial conditions (Eq. 9), resulting in Eqs 26 and 27:

$$A_2 = \frac{V_2 - B}{\omega_d} \quad (26)$$

$$A_3 = \frac{-B}{\omega_d} \quad (27)$$

The rigid body velocity B must still be determined. Substitution of ω^2 (Eq. 19) into the amplitude ratio (Eq. 15), gives the amplitude ratio as a function of m_2 and m_3 :

$$\frac{A_2}{A_3} = -\frac{m_3}{m_2} \quad (28)$$

Substitution of A_3 (Eq. 27) into (Eq. 28) gives A_2 as a function of m_2 , m_3 , ω_d and B :

$$A_2 = \frac{m_3}{m_2} \left(\frac{B}{\omega_d} \right) \quad (29)$$

The rigid-body velocity B is determined by substitution of A_2 from Eq. 29 into Eq. 22, and the initial condition from Eq. 9 for

$\dot{y}_2(0^+) = V_2$, resulting in the rigid body velocity B :

$$B = V_2 \left(\frac{m_2}{m_2 + m_3} \right) \quad (30)$$

The final equations of motion for the anvil table are given by Eqs. 31 through 33 for displacement, velocity and acceleration, respectively:

$$y_2(t) = V_2 \left(\frac{m_2}{m_2 + m_3} \right) \left[\frac{1}{\omega_d} \left(\frac{m_3}{m_2} \right) e^{-\zeta\omega t} \sin(\omega_d t) + t \right] \quad (31)$$

$$\dot{y}_2(t) = V_2 \left(\frac{m_2}{m_2 + m_3} \right) \left[\left(\frac{m_3}{m_2} \right) \omega e^{-\zeta\omega t} \left(\sqrt{1-\zeta^2} \cos(\omega_d t) - \zeta \sin(\omega_d t) \right) + 1 \right] \quad (32)$$

$$\ddot{y}_2(t) = \frac{2V_2\omega}{\sqrt{1-\zeta^2}} \left(\frac{m_3}{m_2 + m_3} \right) e^{-\zeta\omega t} \left[\left(\zeta^2 - \frac{1}{2} \right) \sin(\omega_d t) - \zeta \sqrt{1-\zeta^2} \cos(\omega_d t) \right] \quad (33)$$

The final equations of motion for the equipment are given by Eq. 34 through 36 for displacement, velocity and acceleration, respectively:

$$y_3(t) = V_2 \left(\frac{m_2}{m_2 + m_3} \right) \left[\frac{-1}{\omega_d} e^{-\zeta\omega t} \sin(\omega_d t) + t \right] \quad (34)$$

$$\dot{y}_3(t) = V_2 \left(\frac{m_2}{m_2 + m_3} \right) \left[-\frac{1}{\sqrt{1-\zeta^2}} e^{-\zeta\omega t} \left(\sqrt{1-\zeta^2} \cos(\omega_d t) - \zeta \sin(\omega_d t) \right) + 1 \right] \quad (35)$$

$$\ddot{y}_3(t) = \frac{-2V_2\omega}{\sqrt{1-\zeta^2}} \left(\frac{m_2}{m_2 + m_3} \right) e^{-\zeta\omega t} \left[\left(\zeta^2 - \frac{1}{2} \right) \sin(\omega_d t) - \zeta \sqrt{1-\zeta^2} \cos(\omega_d t) \right] \quad (36)$$

A useful piece of information is the maximum equipment acceleration. This maximum will occur when the time derivative of the equipment acceleration equals zero, given by equation Eq. 37:

$$\frac{d\ddot{y}_3(t)}{dt} = 0 \quad (37)$$

Equation 37 holds for the time that corresponds to:

$$t_{\max \ddot{y}_3} = \frac{1}{\omega_d} \tan^{-1} \left(\frac{(2\zeta^2 - 0.5)\sqrt{1-\zeta^2}}{\zeta(2\zeta^2 - 1.5)} \right) \quad (38)$$

MATLAB Function

A MATLAB function was written to determine the quantities given by equations 19 through 38. In addition, the function determines the shock response spectrum (SRS) of the acceleration time history $\ddot{y}_3(t)$ at the base of the equipment. The user has the option to choose which data fit represented by Eqs. 4, 5 or 6 is to be used in the analysis.

Inputs to the MATLAB function are:

w_2 = weight of anvil table (lb_f)

w_3 = weight of equipment (4,400 lb_f nominal) (lb_f)

N = number of car-building channels (specified by MIL-S-901D⁵ based on weight of equipment and length of Dimension A (Figure 13, sheet 3))

Dim A = Dimension A (defined by MIL-S-901D⁵ (Figure 13, sheet 2) (in))

L = Distance between ship-building channels (50 in for standard test) (in)

h = hammer height above horizontal prior to release (ft)

datafit = 'clements' for NRL Report 7396 fit of table velocity to hammer velocity

= 'fmc' for FMC's data fit of anvil table velocity to hammer velocity

= 'nel' for no energy loss fit of anvil table velocity to hammer velocity

zeta = % of critical damping (fraction)

travel = maximum anvil table travel before machine stops are contacted (in)

SRS_{out} = 'yes' if shock response spectrum at base of equipment is requested; otherwise **SRS_{out}** = 'no'

The MATLAB function calculates the following quantities:

m_2 = mass of anvil table, two shipbuilding channels and 50% of N car-building channels (lb_f-sec²/in)

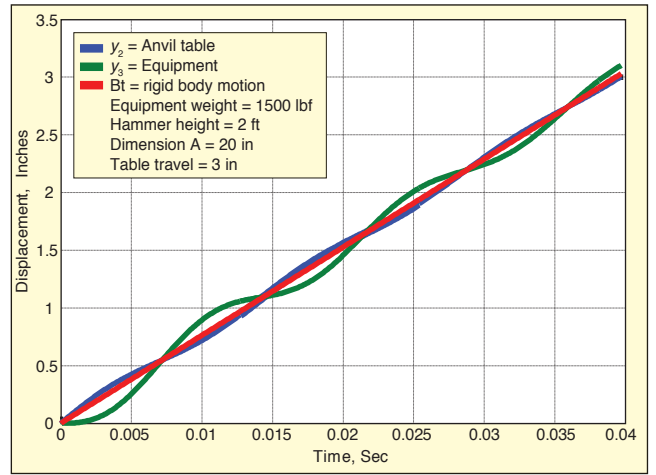


Figure 7. Displacement of equipment, anvil table and rigid-body motion.

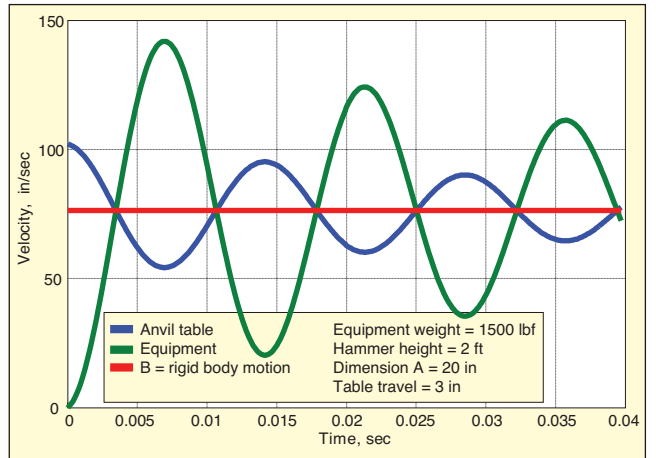


Figure 8. Velocity of equipment, anvil table and rigid-body velocity.

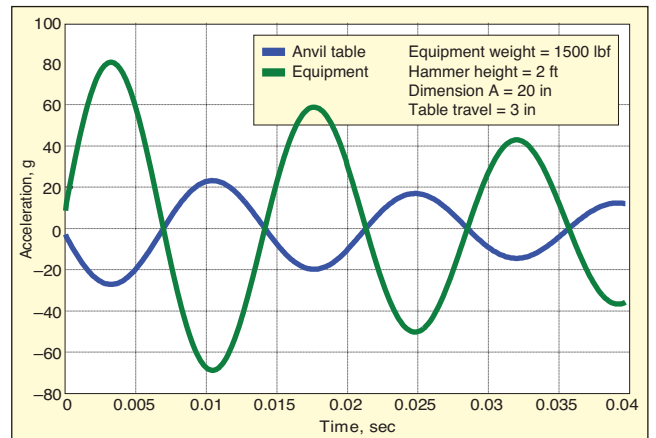


Figure 9. Acceleration of equipment and anvil table.

m_3 = mass of equipment and 50% of N car-building channels (lb_f-sec²/in)

k = system stiffness based on N car-building channels and Dimensions A and L (lb_f/in); note that model assumes equipment CG is symmetrically mounted with respect to shipbuilding channels

ω = nondamped natural frequency for the 2DOF system (rad/sec)

ω_d = damped natural frequency of 2DOF system (rad/sec)

B = rigid-body velocity (in/sec)

y_2 & y_3 = transient displacements of anvil table and equipment, respectively (in)

y_2d & y_3d = transient velocities of anvil table & equipment, respectively (in/sec)

y_2dd & y_3dd = transient accelerations of anvil table and equipment, respectively (in/sec²)

rbm = rigid-body motion displacement Bt (in)

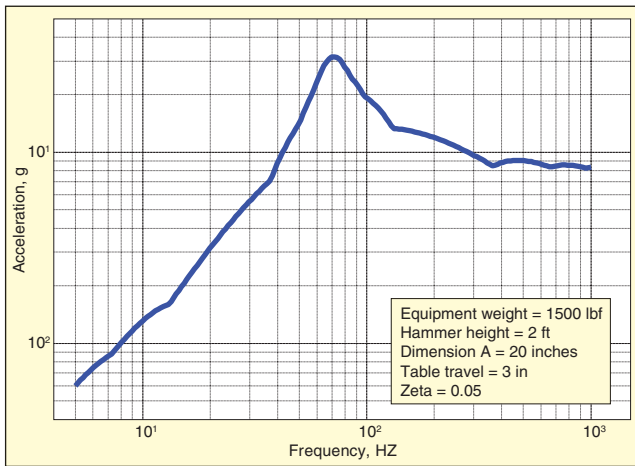


Figure 10. Shock response spectrum from acceleration at base of equipment.

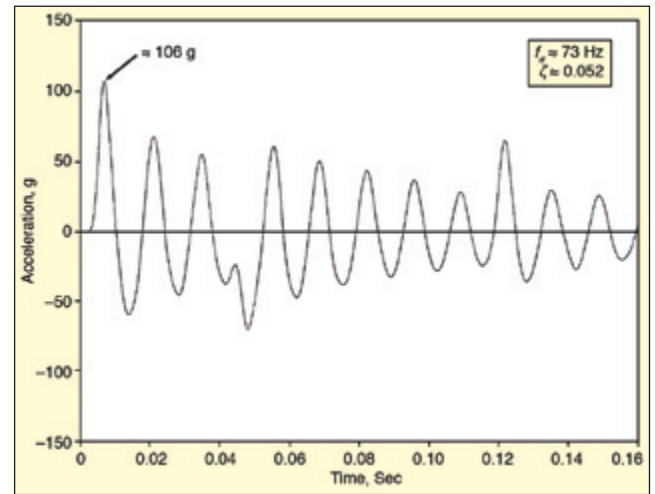


Figure 11. FMC 1,005-lb_f test; accelerometer on top center of test weight.

force = spring (car-building channels) force (lb_f)

MATLAB Function Output for Example Problem

The MATLAB function output from an arbitrary example is plotted in Figures 7 -10; the following parameters were used for this example:

- Equipment weight, 1,500 lbs
- Hammer height, 2 feet
- Dimension A, 20 in
- Table travel, 3 inches
- Datafit, 'nel' (no energy loss)
- Damping, 5% of critical damping

The results of the example are plotted on Figures 7 through Figure 10. Figure 7 shows the displacements of the equipment and the anvil table. The kick-off velocity is evident from the initial positive slope of the anvil table displacement at time = 0. Similarly, the equipment displacement has a horizontal slope at time = 0 consistent with a zero velocity initial condition. The rigid body displacement is given by the red curve indicated by a constant positive slope. During the “up-shock” portion of the event, the equipment and the anvil table oscillate out of phase about the rigid-body displacement. When the anvil table contacts the stops of the machine, 3 inches in this case, the simulation is terminated.

Figure 8 is a plot of the velocity of the anvil table and the equipment velocities oscillating out of phase about the rigid-body velocity. Figure 9 gives the transient acceleration of the anvil table and the equipment. The peak acceleration of the equipment is reached at the first quarter cycle at a time corresponding to Eq.38, 0.00325 seconds in this case. Damping in the model is evident from the displacement, velocity and acceleration plots due to the decreasing amplitudes. Figure 10 is the SRS of the equipment acceleration.

Comparing Analytical Model with FMC MWSM Test Data

FMC did significant testing/characterization of the MWSM in 1990.⁴ A total of 33 individual MWSM hammer strikes were done as a part of that effort. Testing parameters included:

- Test weights (equipment) of 1,005, 2,090, 3,070 and 5,100 pounds
- Dimension A of 30 and 18 inches
- Hammer heights of 1.00, 1.25, 1.50, 2.00, 2.25, 2.50, 3.00, 3.25, 5.00, 5.5 feet
- Table travel of 1.5, 3.0, 3.2 inches

The “equipment” in these tests were slabs of solid steel, not typical compliant shipboard equipment. As such, the lumped mass representation of the equipment in the analytical model is representative of the actual test conditions in this case. Digital data from the FMC testing are no longer available, so the peak acceleration response of the equipment, system frequency and percent of critical damping were determined by approximations made from the physical plots of the test results: Figures 11, 13 and 15. Estimates for system damping were made using the logarithmic decrement method.

Three of the 33 total FMC tests were evaluated with the MATLAB

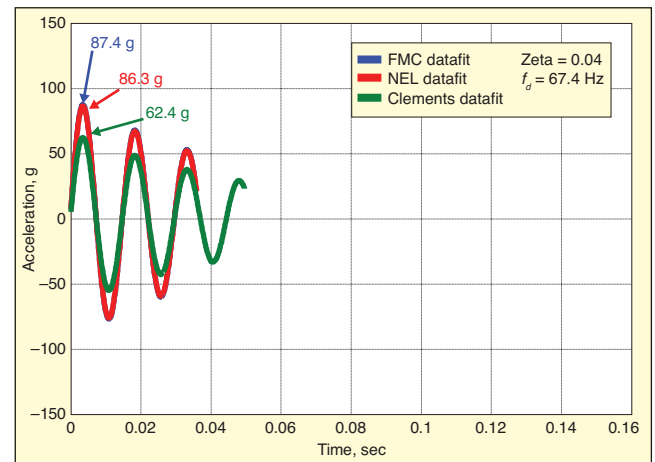


Figure 12. Model 1,005-lb_f analysis.

Table 1. Test and model results – 1,005 lbf weight.

	Peak Acceleration, g	Response Frequency, Hz
FMC Test	106	73
Model, Clements (Eq. 4)	62.4	
Model, FMC (Eq. 5)	87.4	67.4
Model, NEL (Eq. 6)	86.3	

analytical model, representing relatively light, medium and heavy equipment weights of 1005, 3,070 and 5,100 pounds, respectively. In each case, the analytical model results were determined based on each of the three data-fit relationships for hammer impact velocity and anvil table kick-off velocity given by Eqs. 4, 5 and 6. Damping of 4% of critical was assumed for each of the analyses based on information provided in Reference 3.

Light-Weight Equipment Correlation

1,005 pound equipment weight parameters (see Figure 11, Figure 12 and Table 1):

- Equipment weight, 1,005 lb_f
- Dimension A, 18 in
- Hammer height, 2 ft
- Table travel, 3 in
- No. of car-building channels, 3

Medium-Weight Equipment Correlation

3,070 pound equipment weight parameters (see Figure 13, Figure 14 and Table 2):

- Equipment weight, 3,070 lb_f
- Dimension A, 30 in
- Hammer Height, 3 ft

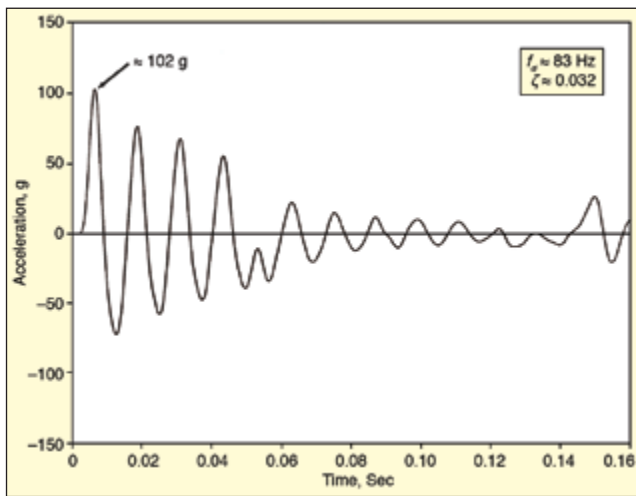


Figure 13. FMC 3,070- lb_f test; accelerometer on top center of test weight.

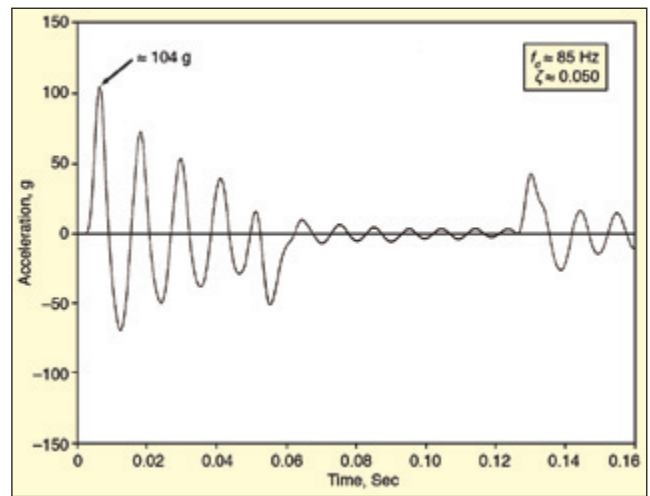


Figure 15. FMC 5,100- lb_f test;; accelerometer on top center of test weight.

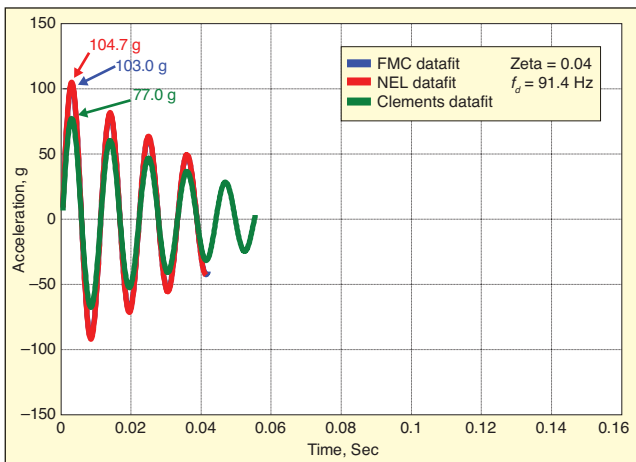


Figure 14. Model 3,070- lb_f analysis..

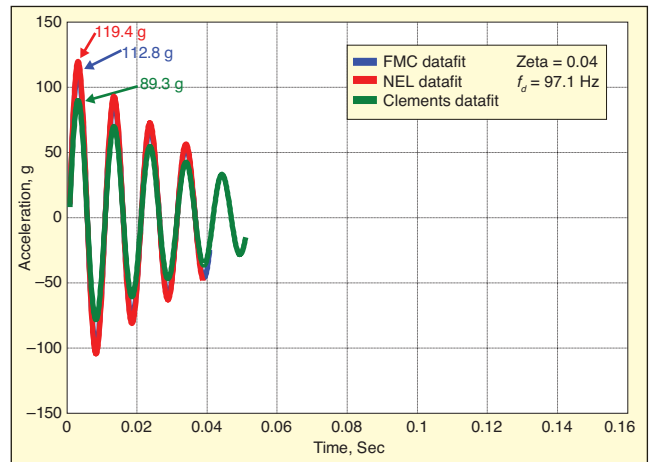


Figure 16. Model 5,100- lb_f analysis.

Table 2. Test and model results – 3,070 lbf weight.

	Peak Acceleration, g	Response Frequency, Hz
FMC Test	102	83
Model , Clements (Eq. 4)	77.0	
Model, FMC (Eq. 5)	103.0	91.4
Model, NEL (Eq. 6)	104.7	

- Table travel, 3 in
- No. of car-building channels, 6

Heavy-Weight Equipment Correlation

5,100 pound equipment weight parameters (see Figure 15, Figure 16 and Table 3):

- Equipment weight, 5,100 lb_f
- Dimension A, 30 in
- Hammer Height, 5.5 ft
- Table Travel, 3 in
- No. Car Building Channels, 9

System-damped frequencies predicted by the analytical model had an average error of 10.7% relative to the FMC test data based on the three cases considered. The individual damped frequency errors ranged from 7.8% understated for the light-weight equipment case to 14.2% overstated for the heavy weight equipment. The peak equipment acceleration average model errors relative to that of the test data were 26.6%, 8.3% and 12.0% for the 'clements' 'fmc' and 'nel' relationships, Eqs. 4, 5 and 6, respectively. For the three cases examined, the model's results for equipment acceleration from the 'fmc' and 'nel' data-fit relationships for anvil table kickoff velocity, Eqs. 5 and 6, were in close agreement. The 'fmc' and 'nel' kickoff velocity relationships resulted in consistently

Table 3. Test and model results – 5,100 lbf weight.

	Peak Acceleration, g	Response Frequency, Hz
FMC Test	104	85
Model , Clements (Eq. 4)	89.3	
Model, FMC (Eq. 5)	112.8	97.1
Model, NEL (Eq. 6)	119.4	

higher, and more accurate peak accelerations for the equipment than that of the Clements velocity relationship.

Conclusions

An analytical model of the MIL-S-901D medium-weight shock machine has been updated to include damping. Testing at the U.S. Naval Research Laboratory and FMC Corp. indicated that damping in the range of 4-5% of critical is present during a test. Equations for equipment and anvil table displacement, velocity and acceleration were updated to include damping. In addition, the relationship between the hammer impact velocity and the anvil table kick-off velocity were further examined beyond the relationship that was published by the Naval Research Lab³ in 1972. Data taken by FMC Corporation⁴ and high speed video taken by BAE Systems resulted in a second relationship (Eq. 5) for anvil table kick-off velocity. A third relationship (Eq. 6) was evaluated based on an assumption of no loss of kinetic energy during the hammer impact with the anvil table.

To facilitate the utility of the updated damped model, a MATLAB function was developed to compute and plot the results of a MWSM test simulation. Equipment transient accelerations from the model were plotted and compared to corresponding data plots from FMC testing.⁴ Three FMC test cases were evaluated with the model for

equipment weights of 1005, 3070 and 5100 pounds. The model average percent error for peak equipment acceleration for the three cases was 9% and 12%, respectively, using the FMC and “no energy loss” anvil table kick-off velocity relationships. Damped frequencies determined by the model for these test weights had errors of 7.7% low, 10.1% high and 14.2% high, respectively, relative to the frequencies determined from test data plots.

While the magnitude of the model errors relative to test data are not insignificant, they are reasonable for an analytical model with only 2 degrees of freedom. If equipment is in preliminary development and ultimately must pass a medium weight shock test, the equipment response predicted by the model can provide an initial estimate of the shock environment as a design guide. Further, the acceleration input or corresponding shock response spectrum determined by the model could be used for input to a more detailed finite-element transient or mode superposition analysis of the equipment. A copy of the MATLAB function can be obtained by contacting the author.

References

1. Welch, W. P., and Saunders, P. D., “Structural and Vibration Analysis of Navy Class High Impact, Medium Weight Shock Tests,” Shock and Vibration Bulletin No. 38, Part 2, pp 95-105, August 1968.
2. Dick, A. F., and Blake, R. E., “Reed-Gage Shock-Spectrum Characteristics of Navy Medium Weight High-Impact Shock Machine,” NRL Report 4750, Naval Research Laboratory, July 10, 1956.
3. Clements, E. W., “Shipboard Shock and Navy Devices for its Simulation,” NRL Report 7396, Naval Research Laboratory, July 14, 1972.
4. Carter, T. L., “Characterize the Shock Environment of the Medium-Weight Shock Machine,” 61 Shock and Vibration Symposium, Pasadena, CA, October 1990.
5. Shock Tests, H. I. (High-Impact) Shipboard Machinery, Equipment, and Systems, Requirements for, MIL-STD-901D (Navy), March 17, 1989.
6. Scavuzzo, R. J., and Pusey, H. C., Naval Shock Analysis and Design, SVM-17, the Shock and Vibration Exchange, HI-TEST Laboratories Inc., 6th printing, 2013. 

The author can be reached at: ed.alexander@baesystems.com.